[redacted]

CAST-86-08
February 1, 1986

CAST-86-08

FERMILAB
FEB 14 1986
LIBRARY

A NEW FORMULATION FOR WAKE POTENTIALS OF A RELATIVISTIC CURRENT IN AN ELLIPTICAL CAVITY+

K. W. Chen and S. H. Kim

Center for Accelerator Science and Technology
University of Texas at Arlington
Arlington, TX 76019

ABSTRACT

A new analytical method to calculate the wake potentials of a bunch of relativistic charged particles in an elliptical cavity is developed by taking the geometry of the pillbox into account prior to the numerical evaluation. Previous formulation of the wake potential is clarified by a proper adaptation of the Floquet theorem and also simplified significantly by decomposing the cavity eigenfunctions into the transverse and longitudinal vector eigenfunctions. Numerical simulations based on the new formulation for the acceleration gradient and the transverse wake potential are presented in terms of driving electron bunches of finite sizes. Typically, for a 1 μC driving charge traversing an elliptical pill-box of 4-mm gap distance, 100 cm^2 in cross section area with a major radius to the minor radius ratio of 2, the accelerating gradient is in excess of 120 MeV/m, while the transverse wake potential at the position of maximum gradient is less than one percent of the accelerating gradient.

ROUTE TO
LOCATION
NAME

+Work supported in part by the Texas Engineering Experiment Station.

(Submitted for publication in Particle Accelerators)

GLOSSARY

$\underset{\sim}{a}_\alpha$	eigenfunctions of the vector potential
c	velocity of light
e	absolute value of the electron charge
dE/dz	acceleration gradient, i.e., energy gain per unit length
$g(s)$	normalized distribution function of the driving bunch
i	$\sqrt{-1}$
$\underset{\sim}{j}$	current density
L	length of the cavity
p	gap distance (height) of the pill-box
Q	charge
r_o	radius of the circular pill-box
S	the cross section of the pill-box
U_z	longitudinal wake potential
$\underset{\sim}{U}_\perp$	transverse wake potential
W_z	the delta-function wake potential
$\underset{\sim}{W}_\perp$	the delta-function transverse wake potential
α	mode number
λ_α	wavelengths of the cavity modes of the vector potential
Ω_α	frequencies of the cavity modes of the scalar potential
ρ	charge density
σ	standard deviation of a Gaussian bunch
ω_α	frequencies of the cavity modes of the vetor potential $\omega_\alpha = c/\lambda_\alpha$
ϕ_α	eigenfunctions of the scalar potential

1. INTRODUCTION

The wake potential of a bunch of relativistic charged particles traversing a cavity consisting of many pill-boxes is of considerable current interest. In general, from the wake potentials, the coupling impedance and energy loss of bunched beams can be evaluated. The idea that the energy lost by the first bunch in a cavity can be utilized as an energy source to accelerate a second trailing bunch of particles has gained further attention.[1] In such a scheme, an extraordinarily large accelerating gradient suitable for next generation particle accelerators could in principle be realized in a two-beam geometry. Recently, several different approaches to calculate the wake potential have appeared in the literature.[1-3] The formulation of the wake potential was shown to be simplified considerably by imposing causality.[1] In this paper we show that these calculations can be further simplified by exploiting the fact that the cavity eigenvectors in the formulation can be decomposed into two categories: longitudinal eigenvectors and transverse eigenvectors. We make additional clarification in the previously ambiguous formulation for the wake potential from the non-rigorous use of Floquet's theorem. Our final formulation yields a form similar to that of the Coulomb law. The effective electric field (accelerating gradient) is found to be inversely proportional to the square of a distance. Using the mode-decomposition and proper use of Floquet's theorem, we reformulate the wake potential in a more convenient form to be more readily calculable numerically. Specifically, we investigate the wake potentials of an elliptic cavity, which is relavent in the design of a wake-field accelerator using elliptical pill-boxes.[4] The use of elliptical wake field cavities permits periodic staging of

acceleration sections not readily adaptable in other equivalent cavity geometries, such as that using annular cross sections. The relative merit and general advantages of using elliptical cavities in a wake-field accelerator scheme under study will be presented elsewhere.

2. THE LONGITUDINAL WAKE POTENTIAL

In this section the wake field potential in a pill-box geometry is formulated in the mode concept. Consider an accelerator cavity consisting of a very large number of elliptic pill boxes. A point charge Q passes through one of the foci of the elliptic disks with a speed c. Let the transverse coordinates of these centers be $\underset{\sim}{r}_\perp = (x_o, 0)$ and $(-x_o, 0)$.

2.1 Mode Analysis

The charge and current density are given by

$$\rho(\underset{\sim}{r}, t) = Q\delta(x - x_o)\delta(y - y_o)\delta(z - ct) \tag{1}$$

and

$$\underset{\sim}{j}(\underset{\sim}{r}, t) = \hat{z}c\rho(\underset{\sim}{r}, t) \quad . \tag{2}$$

The vector and scalar potentials under the Coulomb gauge due to the current and charge sources given by Eqs. (1) and (2), respectively, can be expanded in the Fourier series as

$$\underset{\sim}{A}(\underset{\sim}{r}, t) = \sum_\alpha q_\alpha(t)\underset{\sim}{a}_\alpha(\underset{\sim}{r}) \quad , \tag{3}$$

and

$$\Phi(\underset{\sim}{r}, t) = \sum_\alpha d_\alpha(t)\phi_\alpha(\underset{\sim}{r}) \quad , \tag{4}$$

where $\{\underset{\sim}{a}_\alpha\}$ is the set of normalized vector eigenfunctions given by the following equation and boundary conditions:

$$\nabla^2 \underset{\sim}{a}_\alpha + \frac{\omega_\alpha^2}{c^2} \underset{\sim}{a}_\alpha = 0 \tag{5}$$

and

$$\nabla \cdot \underset{\sim}{a}_\alpha = 0 \tag{6}$$

everywhere, and

$$\underset{\sim}{a}_\alpha \times \hat{n} = 0 \tag{7}$$

on the surface of the metallic enclosure of the accelerator cavity where n is the normal vector of the surface, and $\{\phi_\alpha\}$ is the set of normalized scalar eigenfunctions given by the following equation and boundary condition:

$$\nabla^2 \phi_\alpha + \frac{\Omega_\alpha^2}{c^2} \phi_\alpha = 0 \tag{8}$$

everywhere. Note that

$$0_\alpha = 0 \tag{9}$$

on the surface of the metallic enclosure.

Using Eqs. (1)-(9) and the Maxwell equations, we have, in Gaussian units,

$$q_\alpha(t) = \frac{4\pi c^2 Q}{\omega_\alpha} \int_0^{\min(t,L/c)} \sin\omega_\alpha(t - t') a_{\alpha z}(x_o, 0, ct') dt' \ , \quad \text{for } t > 0$$

$$= 0 \ , \text{ for } t < 0 \ , \tag{10}$$

and

$$r_\alpha(t) = \frac{4\pi c^2 Q}{\Omega_\alpha^2} \phi_\alpha(x_o,0,ct) \ , \quad \text{for } 0 < t < L/c$$

$$= 0 \ , \quad \text{otherwise.} \tag{11}$$

Substituting Eqs. (3), (4), (10), and (11) into $\underset{\sim}{E} = (-1/c)\partial\underset{\sim}{A}/\partial t - \nabla\Phi$, we can express the electric field at any position in the accelerator cavity in terms of the cavity eigenfunctions as

$$\underset{\sim}{E}(r,t) = -4\pi c^2 Q \sum_\alpha \{-\frac{1}{c}\int_0^t dt' \cos[\omega_\alpha(t - t')]a_{\alpha z}(x_o,0,ct')\underset{\sim}{a}_\alpha(\underset{\sim}{r}) +$$

$$+ \frac{1}{\Omega_\beta^2} \phi_\alpha(x_o,0,ct)\nabla\phi_\alpha(\underset{\sim}{r})\} \qquad \text{for } t < L/c \ ,$$

and

$$\underset{\sim}{E}(r,t) = 0 \quad \text{for } t < 0. \tag{12}$$

2.2 Delta-function Longitudinal Wake Potential

The delta-function longitudinal wake potential W_z is defined as the energy gained by a unit negative point charge with a velocity c traveling in the path passing through the other elliptic centers, at a distance s in the z direction behind the accelerating point charge Q. Thus,

$$W_z(s) = -\int_0^L dz \ E_z(-x_o,0,z,(z+s)/c) \quad . \tag{13}$$

Since a signal cannot travel faster than the speed of light and the point charge is assumed to move with the speed of light, the energy loss of the driving electron bunch is independent of the aperture size. Substituting Eq. (12) into Eq. (13), we obtain for $0 < s < L$

$$W_z(s) = 4\pi Q \sum_\alpha \{(\int_0^{L-s} \int_0^{z+s} + \int_{L-s}^{L} \int_0^{L}) \, dz \, dz' \, a_{\alpha z}(-x_o,0,z)$$

$$\times \cos[\omega_\alpha(z + s - z')/c] a_{\alpha z}(x_o,0,z') + \frac{c^2}{\Omega_\alpha^2} \int_0^{L-s} dz \, \phi_\alpha(x_o,0,z+s) \frac{\partial 0_\alpha}{\partial z}(-x_o,0,z)\} \, . \tag{14}$$

We impose the causality on Eq. (14)[1], yielding the result given by

$$W_z(s) = 4\pi Q \sum_\alpha \left| \int_0^L a_\alpha(z) \exp(i\omega_\alpha z/c) dz \right|^2 \cos(\omega_\alpha s/c) \quad . \tag{15}$$

Since the acceleration cavity is a repeating structure with period p, $a_\alpha(z)$ is required by Floquet's periodicity theorem to satisfy

$$a_\alpha(z + np) = e^{in\beta} a_\alpha(z) \, , \tag{16}$$

where β should be determined by the physical conditions on $W_z(s)$. Since the cavity is assumed to be lossless, β should be real. We then have

$$\int_0^L a_\alpha(z) \exp(i\omega_\alpha z/c) dz = \int_0^L a_\alpha(z) \exp(i\omega_\alpha z/c) dz \sum_{n=0}^{n_o} \exp[i(\beta_\alpha + \omega_\alpha p/c)n] \, , \tag{17}$$

where $n_o = L/p - 1$. Since $W_z(s)$ is proportional to L, β_α must be equal to $-\omega_\alpha p/c$ in the proper (rigorous) use of Floquet's theorem. Substituting $\beta_\alpha = -\omega_\alpha p/c$ into Eq. (17) and combing the resulting equation with Eq. (15), we obtain the longitudinal wake potential per unit length (or the acceleration gradient, which is simply called the longitudinal wake potential in Ref.1. We adopt the same nomenclature as Ref. 1) as

$$\frac{W_z}{L} = \frac{4\pi Q}{p^2} \sum_\alpha V^*_\alpha(x_o,0,\lambda_\alpha)V_\alpha(-x_o,0,\lambda_\alpha)\cos(s/\lambda_\alpha) \quad , \tag{18}$$

where

$$V_\alpha(x,y,\lambda_\alpha) = \int_0^1 a^p_{\alpha z}(x,y,z)\exp(iz/\lambda_\alpha)dz \quad . \tag{19}$$

Here, all distances such as z and λ_α are measured in units of the pillbox gap p, and

$$\nabla^2 \underset{\sim}{a}^p_\alpha + \frac{1}{\lambda_\alpha^2}\underset{\sim}{a}^p_\alpha = 0 \quad , \tag{20}$$

and

$$\iiint_{V_p} \underset{\sim}{a}^p_\alpha \cdot \underset{\sim}{a}^p_\beta \, d^3r = \delta_{\alpha,\beta} \quad , \tag{21}$$

where V_p denotes the space in the pillbox.

Since the driving electrons are distributed over a finite length in the z direction, we define the wake potential in terms of the delta-function wake potential as

$$U_z = \int_{-s}^{\infty} W_z(s + s')g(s')ds' \quad , \tag{22}$$

where $g(s')$ is the normalized distribution function of the driving charge.

3. THE TRANSVERSE WAKE POTENTIAL

Consider again the exciting charge Q traveling the one foci of the elliptic cavity at v = c. The delta-function transverse wake potential $\underset{\sim}{W}_\perp$ is defined as the transverse momentum kick experienced by a test charge following at a distance s in the z direction on the other foci and also at v = c. Thus,

$$\underset{\sim}{W}_\perp(s) = \int_0^L [\underset{\sim}{E}_\perp + (\underset{\sim}{v} \times \underset{\sim}{B})_\perp/c]_{t=(z+s)/c} dz$$

$$= \int_0^L [\nabla_\perp A_z - \nabla_\perp \Phi]_{t=(z+s)/c} dz + \underset{\sim}{A}_\perp \Big|_{z=0,\,t=s/c}^{z=L,\,t=(L+s)/c}$$

$$= \int_0^L [\nabla_\perp A_z - \nabla_\perp \Phi]_{t=(z+s)/c} \quad . \tag{23}$$

Here, Eq. (7) has been used to eliminate the last term in the second equation. Analogously to the longitudinal case, Eq. (23) can, by using the casuality, periodicity, and the geometic property of the pillbox being a right cylinder whose axis is aligned with the z axis, be reduced to

$$\frac{\underset{\sim}{W}_\perp(s)}{L} = \frac{4\pi Q}{p^2} \sum_\alpha V_\alpha^*(x_o,0,\lambda_\alpha)\nabla_\perp V_\alpha(-x_o,0,\lambda_\alpha)\lambda_\alpha \sin(s/\lambda_\alpha) \quad , \tag{24}$$

where $V_\alpha(\lambda_\alpha)$ and λ_α are defined by Eqs. (19)-(21). Similar to Eq. (22), the transverse wake potential or the transverse momentum kick experienced by a unit negative charge following a distance s in the z direction behind the driving charge bunch of an arbitrary charge distribution on the path passing

through other foci of the elliptical pill boxes is defined by

$$\underset{\sim}{U}_{\perp}(s) = \int_{-s}^{\infty} \underset{\sim}{W}_{\perp}(s + s')g(s')ds' \quad , \tag{25}$$

where g(s) is the charge distribution of the driving bunch.

4. MODE DECOMPOSITION OF THE WAKE POTENTIALS

For an elliptic pillbox with an geometry shown in Figure 1, the cavity vector eigenfunctions $\mathbf{a} = a_x x + a_y y + a_z z$ should satisfy the following equations and boundary conditions:

$$\nabla^2 a_x + a_x/\lambda^2 = 0 \quad , \tag{26}$$

$$\nabla^2 a_y + a_y/\lambda^2 = 0 \tag{27}$$

in the pillbox,

$$a_x = a_y = 0 \text{ at } z = 0 \text{ and } z = 1, \tag{28}$$

$a_x/a_y = y_b^2 x/x_b^2 y$ for (x,y) on the periphery of the elliptic cross section given by $x^2/x_b^2 + y^2/y_b^2 = 1$, (29)

$$\nabla^2 a_z + a_z/\lambda^2 = 0 \tag{30}$$

in the pillbox,

$a_z = 0$ for (x,y) on the periphery of the elliptic cross section, (31)

and

$$\nabla \cdot \underset{\sim}{a} = 0 \quad . \tag{32}$$

Because the boundary conditions on a_x, a_y, and a_z are different, they cannot generally have the same eigenvalues. Consequently the cavity eigenvetors divide themselves into two categories:

4.1 Longitudinal Eigenvector

$\underset{\sim}{a} = a_z \hat{z}$ where a_z should satisfy Eqs (30)-(31). Note that the longitudinal eigenvetor $\underset{\sim}{a}$ satisfy Eqs. (26)-(32).

4.2 Transverse Eigenvector

$\underset{\sim}{a} = a_x \hat{x} + a_y \hat{y}$ where a_x and a_y should satisfy Eqs. (23)-(26) simultaneously. Of course, these longitudinal eigenvectors satisfy Eqs. (26)-(32) simultaneously. Since the transverse eigenvectors do not contribute to either the longitudinal or the transverse wake potential, we need not calculate them here (however, these transverse eigenvectors are related to the energy loss of the driving charge). Because of Eq. (32), the longitudinal eigenvectors have the form

$$\underset{\sim}{a} = f(x,y)\ \hat{z} \quad , \tag{33}$$

where c and f(x,y) are determined by

$$\nabla_\perp^2 f(x,y) + f(x,y)/\lambda^2 = 0 \quad , \tag{34}$$

$$f(x,y) = 0 \quad \text{for } (x,y) \text{ such that } x^2/x_b^2 + y^2/y_b^2 = 1 \quad , \tag{35}$$

and

$$\iint_{S_p} f^2(x,y)\,dxdy = 1 \quad , \tag{36}$$

where S_p is the cross section of the pillbox.

4.2.1 Circular Cylindrical Cavity

Using the above formulation, we first obtain an analytical estimation of

the delta-function wake potential for a wake field cavity using pill boxes having a circular cross section, and subsequently outline a numerical method based on Galerkin's method.[7]

For a circular cross section with radius r_o, $\underset{\sim}{W}_\perp = 0$. We readily obtain

$$\frac{W_z(s)}{L} = \frac{8Q}{p^2} \sum_n [1 - \cos(\xi_n/r_o)]\cos(s\xi_n/r_o)/J_1^2(\xi_n)\xi_n^2 \quad , \qquad (37)$$

where $J_1(\xi)$ is the Bessel function of order 1, ξ_n is the n-th root of $J_0(\xi) = 0$, and r_o and s are measured in units of p.

Delta-function Driving Bunch

The delta-function wake potential from the lowest mode, which makes the dominant contribution, is given by

$$W_z(s)/L = 5.2 \frac{Q}{p^2}[1 - \cos(2.43/r_o)]\cos(2.43s/r_o)$$

$$= 50 \frac{Q}{S^2}\cos(4.3s/S^{1/2}) \quad \text{for } r_o/2.43 \gg 1 \quad , \qquad (38)$$

where S is the actual cross section of the pillbox. We identify two salient features: (1) the smaller the pillbox gap p, the greater the acceleration gradient. (2) the greater the radius of the cross section of the pillbox, the greater the oscillation period of the delta-function wake potential. However, the greater the radius, the smaller is the acceleration gradient (this is due to the fact that the energy radiated from the driving charge should spread over all pillbox space). Since the lengths of both the driving electron

bunch and accelerated electron bunch are much larger than the pill box gap, it is understood by Eq.(34) that the radius should be much greater than p. For a typical example in which $r_o = 8$ (the actual radius = 3.2 cm), p = 4 mm, and Q = 1 μC, the acceleration gradient is shown to be of the order of 137 MeV/m. Note that this value is a lower limit estimate which does not include the contributions from higher modes.

Gaussian Driving Bunch

If the driving electron bunch has a Gaussian distribution given by

$$g(z) = \frac{1}{(2\pi)^{1/2}\sigma}\exp\left(-\frac{z^2}{2\sigma^2}\right) \quad , \tag{39}$$

the acceleration gradient for an electron is, for $s \gg \sigma$

$$\frac{dE}{dz} = 50\,\frac{Qe}{S^2}\exp\left(-\,9.2\frac{\sigma^2}{S^2}\right) \quad , \tag{40}$$

where $e = -|e|$, and

$$(2\pi)^{-1/2}\sigma^{-1}\int_{-\infty}^{\infty}\exp(-x^2/2\sigma^2)\cos[(s + x)/\lambda]dx = \exp(-\sigma^2/2\lambda^2)\cos(s/\lambda) \tag{41}$$

has been used. From Eq. (40), we clearly understand that the size of the driving electron bunch should be much smaller than the radius of the cross section. An electron at the center of the driving electron bunch is decelerated, and the magnitude of the deceleration gradient at the center, i.e.,

$$(2\pi)^{-1/2}\sigma^{-1}L^{-1}\int_0^\infty eW_z(s + x)\exp(-x^2/2\sigma^2)dx$$

is exactly half of the maximum acceleration gradient for $s \gg \sigma$. This confirms that the transformation ratio of a device in which both driving and accelerated beams traverse the cavity along the same path cannot be much greater than two for symmetric bunches.[1,5] For asymmetric bunches, it was shown that the transformer ratio can be much greater than two even for a single mode cavity.[6]

4.2.2 Elliptical Cylindrical Cavity

If the cross section becomes elliptic, the transverse wake potential becomes especially important. To calculate the longitudinal and transverse wake potentials in the elliptic geometry, we first note that the solution $f(x,y)$ of Eqs. (34) and (35) should be an even or odd function with respect to both x and y: $f(x,y)$ cannot have a mixed parity. We readily find that the odd functions with respect to y do not contribute to either the longitudinal wake potential or the transverse momentum kick since the value of such a function at $y = 0$ is zero. Therefore, an appropriate form for an approximation of $f(x,y)$ can be either

$$f_{even}(x,y) = C(x^2/x_b^2 + y^2/y_b^2 - 1)\sum_{i,j} f_{even}(i,j)x^{2i}y^{2j} \quad , \qquad (42)$$

or

$$f_{odd}(x,y) = C(x^2/x_b^2 + y^2/y_b^2 - 1)\sum_{i,j} f_{odd}(i,j)x^{2i+1}y^{2j} \quad , \qquad (43)$$

where C is a constant which is determined by the normalization condition given by Eq. (38). Then, the Galerkin's method is to let $\nabla_\perp^2 f(x,y) + f(x,y)/\lambda^2$ be orthogonal to a suitably chosen set of basis functions. For example, to make $f_{even}(x,y)$ be orthogonal to all $u_{1,0}(x,y)= x^2$, $u_{0,1}(x,y)=y^2$, $u_{1,1}(x,y) = x^2y^2$, $u_{0,2}(x,y) = x^4$, ... Therefore, according to the present method, the mode-analysis reduces to a standard eigenvalue-eigenvector problem, i.e.,

$$\overleftrightarrow{A}\cdot\underset{\sim}{f}_{even} = -(1/\lambda^2)\overleftrightarrow{B}\cdot\underset{\sim}{f}_{even} \quad , \tag{44}$$

where

$$\underset{\sim}{f}_{even} = \begin{pmatrix} f_{even}(0,0) \\ f_{even}(0,1) \\ f_{even}(1,0) \\ \cdot \\ \cdot \\ \cdot \end{pmatrix} \quad , \tag{45}$$

the (mn),(ij) elements of the matrices A and B are, respectively

$$A_{(mn),(ij)} = \iint_{V_p} \{[2i(2i-1)x^{2i-2}y^{2j} + 2j(2j-1)x^{2i}y^{2j-2}]E(x,y) + 2x^{2i}y^{2j}(1/x_b^2 + 1/y_b^2) + 8(i/x_b^2 + j/y_b^2)x^{2i}y^{2j}\}x^{2m}y^{2n}\,dxdy \quad , \tag{46}$$

and

$$B_{(mn),(ij)} = \iint_{V_p} x^{2i}y^{2j}E(x,y)x^{2m}y^{2n}\,dxdy \quad , \tag{47}$$

with $E(x,y) = x^2/x_b^2 + y^2/y_b^2 - 1$.

Accordingly, the acceleration gradients and the transverse momentum kicks per unit length experienced by the electron on the same path as that of the driving Gaussian bunch and the electron on the path passing through the other foci of pill boxes are given by, for $s \gg \sigma$

$$\frac{dE}{dz} = \frac{8\pi Qe}{p^2} \sum_{\alpha} \{|f_{\alpha,even}(x_o,0)|^2\lambda_\alpha^2[1 - \cos(1/\lambda_\alpha)]\exp(-\sigma^2/2\lambda_\alpha^2)\cos(s/\lambda_\alpha)$$

$$\pm |f_{\alpha,odd}(x_o,0)|^2\lambda_\alpha^2[1 - \cos(1/\lambda_\alpha)\exp(-\sigma^2/2\lambda_\alpha^2)\cos(s/\lambda_\alpha)\}$$

$$= \frac{8\pi Qe}{p^2}(x_o^2/x_b^2 - 1)^2 \sum_{\alpha} \{[\sum_{i=0} f_{\alpha,even}(i,0)x_o^{2i}]^2\lambda_\alpha^2[1 - \cos(1/\lambda_\alpha)]$$

$$\times \exp(-\sigma^2/2\lambda_\alpha^2)\cos(s/\lambda_\alpha) \pm [\sum_{i=0} f_{\alpha,odd}(i,0)x_o^{2i+1}]^2\lambda_\alpha^2[1 - \cos(1/\lambda_\alpha)]$$

$$\times \exp(-\sigma^2/2\lambda_\alpha^2)\cos(s/\lambda_\alpha)\} \quad , \tag{48}$$

and

$$\frac{U_x(z)}{L} = \frac{8\pi Qe}{p^2} \sum_{\alpha} \{\pm f_{\alpha,even}(x_o,0)\frac{\partial f_{\alpha,even}(x_o,0)}{\partial x}\lambda_\alpha^3[1 - \cos(1/\lambda_\alpha)]$$

$$\times \exp(-\sigma^2/2\lambda_\alpha^2)\sin(s/\lambda_\alpha) + f_{\alpha,odd}(x_o,0)\frac{\partial f_{\alpha,odd}(x_o,0)}{\partial x}\lambda_\alpha^3[1 - \cos(1/\lambda_\alpha)]$$

$$\times \exp(-\sigma^2/2\lambda_\alpha^2)\sin(s/\lambda_\alpha)\}$$

$$= \frac{8\pi Qe}{p^2}(x_o^2/x_b^2 - 1) \sum_\alpha \{\pm[\sum_{i=0} f_{\alpha,even}(i,0)x_o^{2i}][\frac{2x_o}{x_b^2} f_{\alpha,even}(0,0) +$$

$$+ (\frac{3x_o^2}{x_b^2} - 1) \sum_{i=1} f_{\alpha,even}(i,0)x_o^{2i-1}]\lambda_\alpha^3[1 - \cos(1/\lambda_\alpha)]\exp(-\sigma^2/2\lambda_\alpha^2)\sin(s/\lambda_\alpha)$$

$$+ (\frac{3x_o^2}{x_b^2} - 1)[\sum_{i=0} f_{\alpha,odd}(i,0)x_o^{2i+1}][\sum_{i=0} f_{\alpha,odd}(i,0)x_o^{2i}]\lambda_\alpha^3$$

$$\times [1 - \cos(1/\lambda_\alpha)]\exp(-\sigma^2/2\lambda_\alpha^2)\sin(s/\lambda_\alpha)\} \quad , \qquad (49)$$

where the upper and lower signs of "$\pm$" apply to the accelerated electron on the same path ($x = x_o$, $y = 0$) as the driving bunch and the other path ($x = -x_o$, $y = 0$), respectively.

Using the method developed, we present numerical simulations to determine some salient features of an elliptical pill-box cavity in the next section.

5. NUMERICAL SIMULATION RESULTS

We first show results for a circular cross section found in the usual collinear configuration, followed by those for elliptic cross sections. The circular cross section is a limiting case of the elliptical cross section in which x_b becomes equal to y_b.

Figure 2 shows the curves of the longitudinal wake potential computed by the numerical method for a pill-box of a circular cross section for different values of the parameter n. Here, n is the parameter describing the number of modes, whose contributions are taken in the summation of Eq. (37). These curves show that the summation of the contributions from modes converges as n increases (contributions from high modes make only small ripples) meaning that we can neglect contributions from modes with mode numbers greater than ten (10) even for a lossless cavity. For cavities with losses, higher-number modes damp faster so that we need not include these modes for the wake potential at s much greater than 1 (or the distance between the centers of the driving and accelerated bunches much greater than the pill-box gap, p).

Figure 3 compares the longitudinal wake potentials, computed by the analytical formulation given by Eq. (37), with that by numerically evaluating $f_\alpha(i,j)$ and λ_α in Eq. (49) for a pill-box of a circular cross section. For easy comparision, only two modes (the principal and second modes) are included in both calculations. We find that both calculations agree with each other. The curves confirm that the result from the numerical method agrees with the result from the analytical formulation, which is readily obtained for the case of the pill-box of circular cross section. It suggests that the present

numerical method can yield accurate results for pill-boxes of elliptical cross section.

Figures 4 and 5 show the longitudinal and transverse wake potentials, respectively for several values of parameter σ, which represent the length of the driving Gaussian bunch. We readily find that both potentials decreases as the length increases for a fixed value of total driving charge.

Figures 6 and 7 show the longitudinal and transverse wake potentials, respectively for several values of y_b/x_b, which designates the elongation of the elliptical cross section (e.g., $y_b/x_b = 1$ for circular cross section and $y_b/x_b = 0$ for line cross section) with all other parameters being fixed. We readily find that the transverse wake potential decreases as y_b/x_b approaches 1 (circular cross section) as expected. However, we also find that the maximum longitudinal wake potential does not become maximum at the values of $y_b/x_b = 1$ (circular cross section), indicating that an elliptic cross section has a larger acceleration gradient than the circular cross section. The acceleration gradient can be greater than 100 MeV/m for a total driving charge of 1 μC, pill-box gap of 4 mm, and an elliptical cross section of $x_b = 8$ cm and y_b=4 cm.

Figure 8 shows both the longitudinal and transverse potentials versus the distance between the centers of driving and accelerated charges, s. These curves clearly reveal that we can find a position at which the the acceleration gradient (the longitudinal wake potential) becomes maximum while the mometum kick (the transverse wake potential) becomes negligible for elliptic pill-boxes.

6. CONCLUSION AND DISCUSSION

It is well known that the formulation of the wake potentials of a relativistic current in a cavity can be simplified by imposing the causality and using Floquet's theorem for periodic boundary conditions. However, previous formulation is ambigous due to a nonrigorous use of Floquet's theorem, which is clarified in this paper. The formulation is simplified further by utilizing the fact that the cavity eigenmodes naturally decompose into two distinctive categories: longitudinal and transverse modes. We calculate numerically the wake potentials for elliptic pill-boxes for the new formulation. Numerical calculations reveal two salient features: (i) The maximum of the magnitude of the acceleration gradient is not achieved with a circular cross section for a given set of parameters such as the total charge and length of driving bunch, pill-box gap, and the major radius; in fact, elliptical cross section is better suited than the circular cross section as far as the magnitude of the acceleration gradient is concerned. (ii) A position can be found at which the acceleration gradient becomes maximum while the momentum kick becomes negligible. This point is especially important in the optimum design of a wake-field accelerator based on the use of elliptical cavities. The acceleration gradient can easily exceed 100 MeV/m for a driving charge of 1 μC traversing a standard elliptical pill-box.

AKNOWLEDGMENT

It is pleasure to acknowledge the assistance of computer simulation by Prof. Z. Chen.

REFERENCES

1. K. L. F. Bane, P. B. Wilson, and T. Weiland, Physics of High Energy Particle Accelerators, AIP Conf. Proc. No. 127, edited by M. Month, P. F. Dahl, and M. Dienes (AIP, New York, 1983), p. 876

2. T. Weiland and B. Zotter, Particle Accelerators, 2, 143 (1981).

3. P. L. Morton, V. K. Neil, and A. M. Sessler, J. Appl. Phys. 37, 3875 (1966).

4. K. W. Chen and S. H. Kim, CAST-85-25, Center for Accelerator Science and Technology, University of Texas at Arlington (1985) (Unpublished).

5. J. Seeman, IEEE Trans. Nucl. Sci. NS-30, 3180 (1983).

6. K. L. F. Bane, P. Chen, P. B. Wilson, IEEE Trans. Nucl. Sci. NS-32, 3524 (1985).

7. J. J. Conner and C. A. Brebbia, Finite Element Techniques for Fluid Flow (Newnes-Butterworths, London, 1976), p. 7.

FIGURE CAPTIONS

FIGURE 1 Cross section of a two-beam elliptical pill-box. x_b and y_b are measured in units of the pill-box gap (or height), p.

FIGURE 2 Plots of the longitudinal wake potential of a Gaussian bunch vs s obtained by the numerical method for $\sigma = 1$, $Q = 1$ μm, $p = 4$mm, a circular cross section with radius $r_o = 20$, and $n = 10$ and 15. Here, n is the number of modes which are taken from the lowest mode, and the potential scale is relative.

FIGURE 3 Plots of the longitudinal wake potential of a Gaussian bunch vs s for $\sigma = 1$, $Q = 1$ μC, $p = 4$mm, a circular cross section with radius $r_o = 20$. Potential scale is relative, and only the principal and second modes are included in both calculations.

FIGURE 4 Plots of the longitudinal wake potentials of Gaussian bunches with $\sigma = 0$ (delta-function wake potential), 1, 2, and 3 vs s for $Q = 1$ μC, an elliptical cross section with major radius $x_b = 20$, minor radius $y_b = 10$, and $p = 4$ mm. Six even modes and six odd modes from the lowest mode were included in this calculation. Potential scale is relative.

FIGURE 5 Plots of the x-component of each transverse wake potential of each Gaussian bunch of each $\sigma = 0$ (delta-function wake potential), 1, 2, and 3 vs s for Q = 1 μC, an elliptical cross section with major radius $x_b = 20$, minor radius $y_b = 10$, and p = 4 mm. Six even modes and six odd modes were included in this calculation. Potential sale is relative.

FIGURE 6 PLots of the logitudinal wake potentials vs s for $\sigma = 1$, Q = 1 μC, p = 4mm, and elliptical cross sections of $x_b = 20$, and $y_b = 0.1, 1, 5, 10, 15$, and 20. $x_b = y_b = 20$ corresponds to a geometry of circular cross section.

Figure 7 Plots of the transverse wake potential vs s for $\sigma = 1$, Q = 1 μC, p = 4mm, and elliptical cross sections of $x_b = 20$, and $y_b = 0.1, 1, 5, 10, 15$, and 20. Potential scale is relative.

Figure 8 Plots of both longitudinal and transverse wake potentials vs s for $\sigma = 1$, Q = 1 μC, p = 4 mm, and elliptical cross section of $x_b = 20$ and $y_b = 10$.

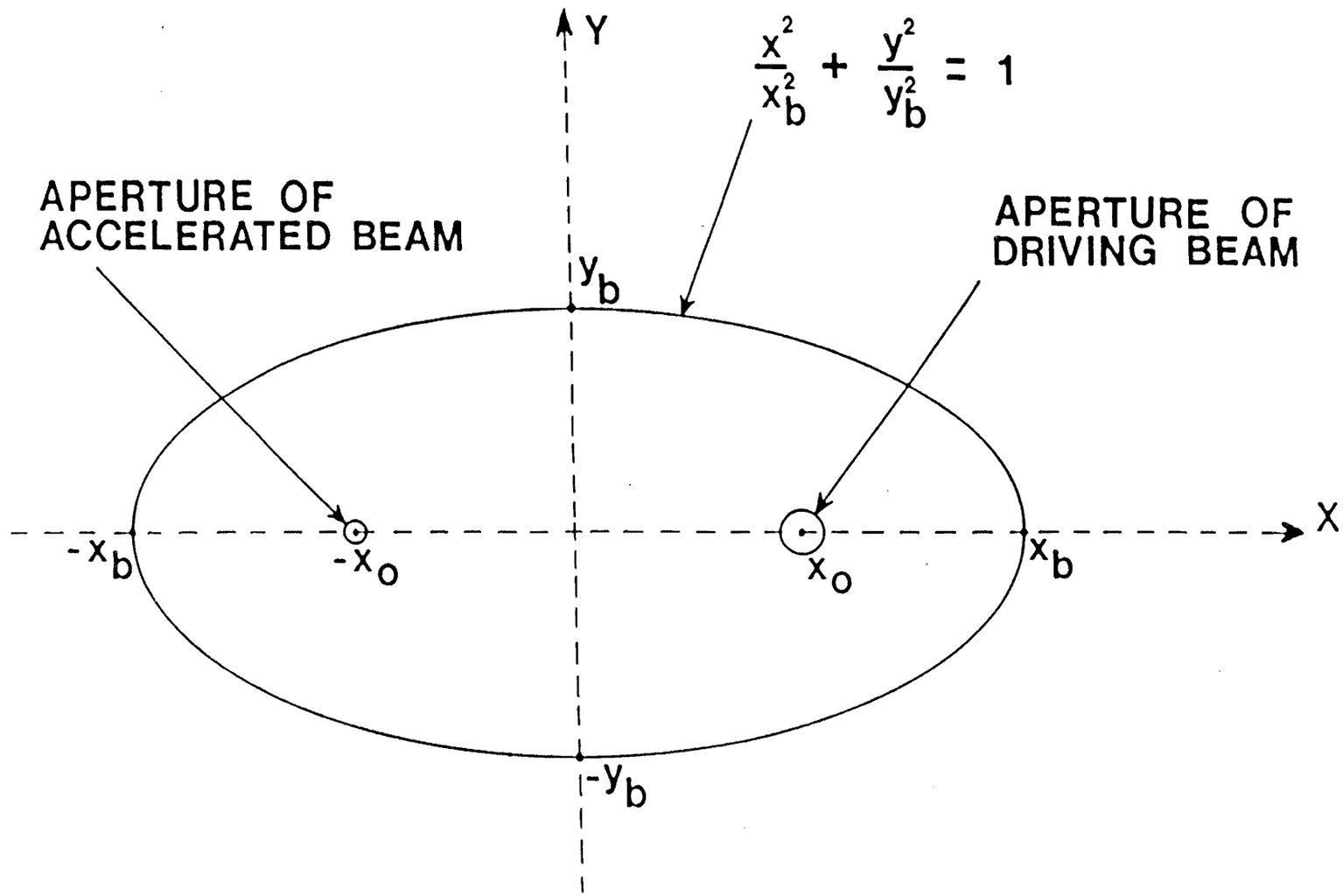

$$x_o = \sqrt{x_b^2 - y_b^2}$$

Fig. 1

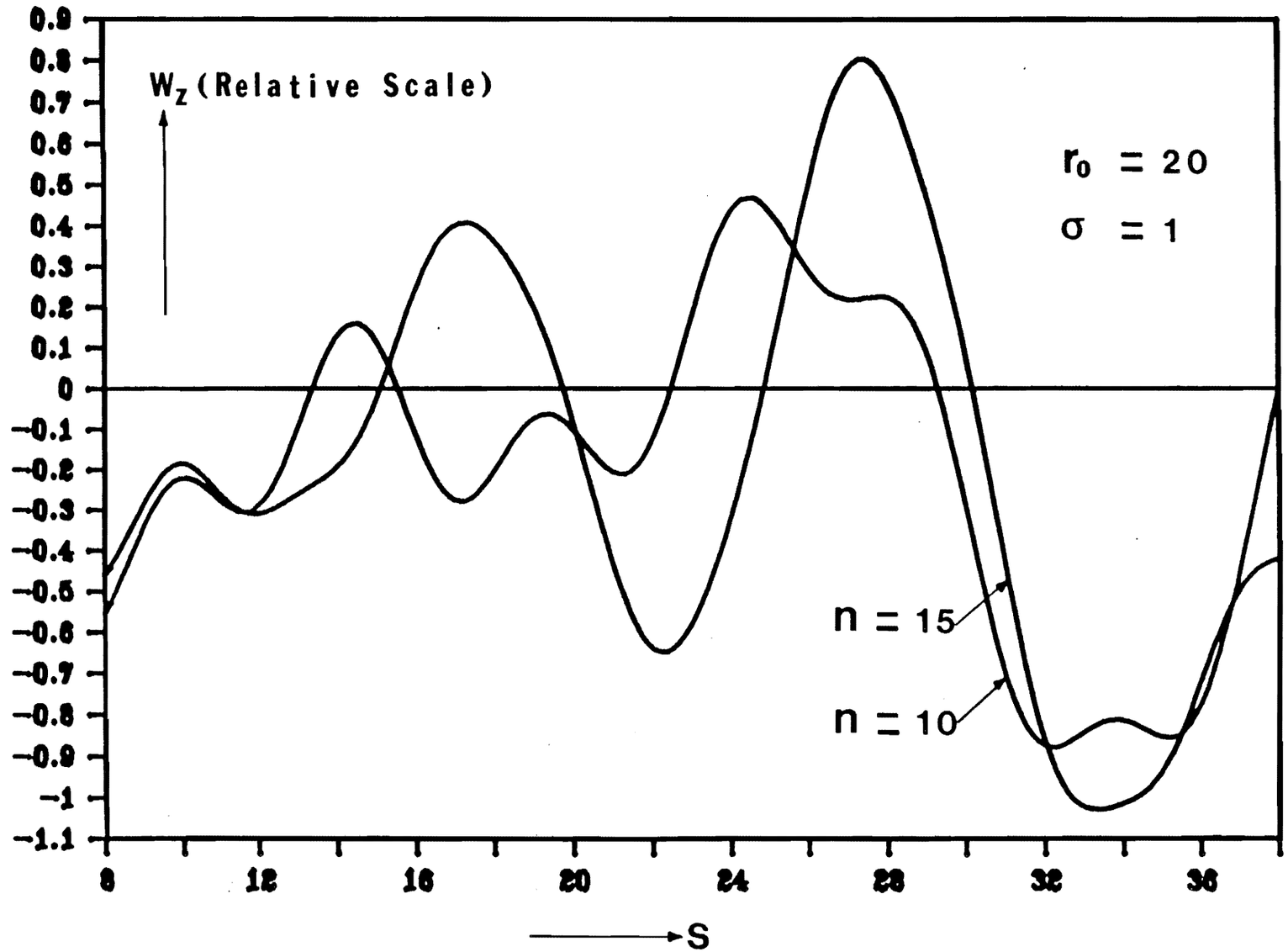
W_z (Relative Scale)
$r_0 = 20$
$\sigma = 1$
n = 15
n = 10
0.9
0.8
0.7
0.6
0.5
0.4
0.3
0.2
0.1
0
−0.1
−0.2
−0.3
−0.4
−0.5
−0.6
−0.7
−0.8
−0.9
−1
−1.1
8
12
16
20
24
28
32
36
S

Fig. 2

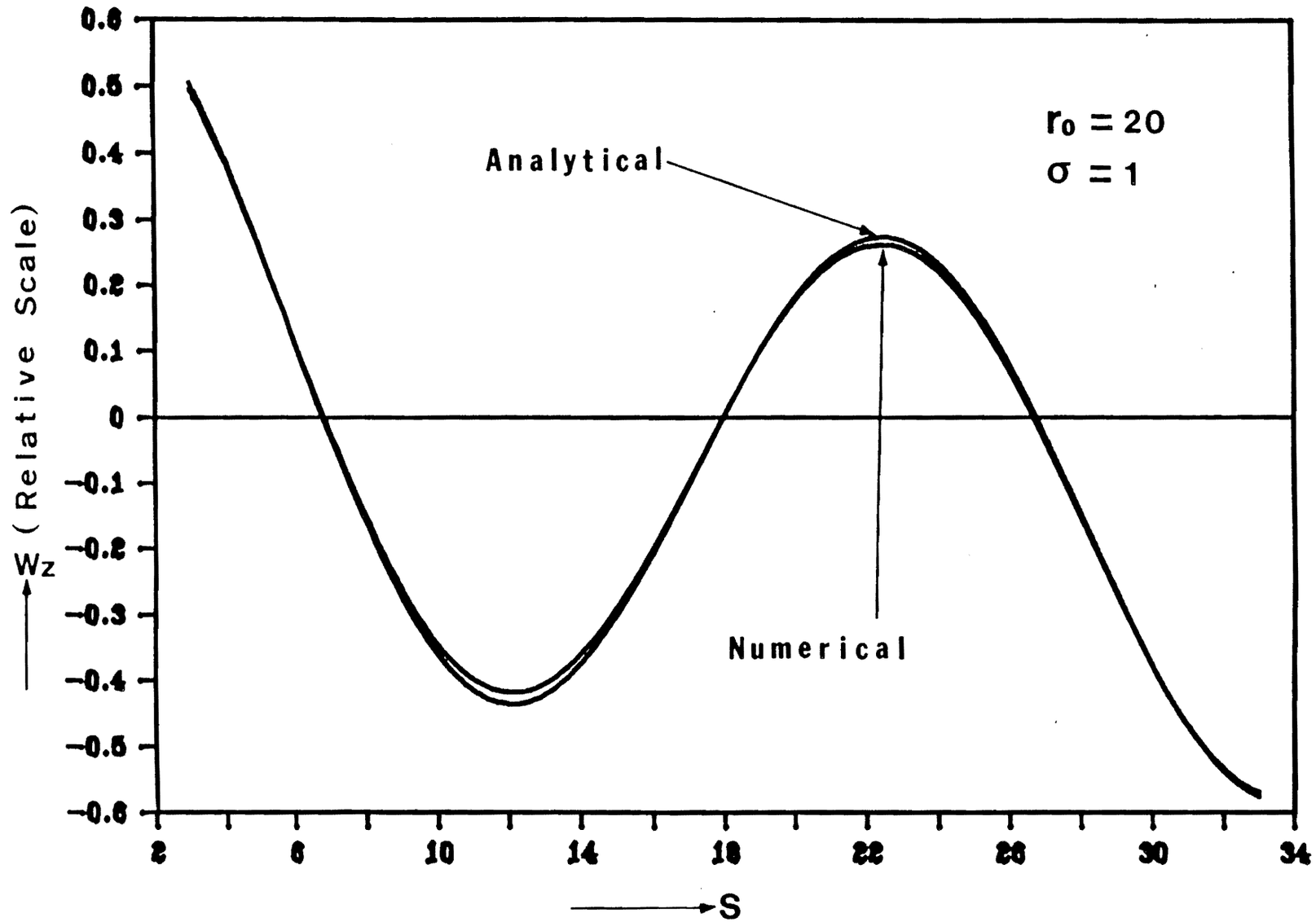
0.6
0.5
0.4
0.3
0.2
0.1
0
-0.1
-0.2
-0.3
-0.4
-0.5
-0.6
Wz (Relative Scale)
2
6
10
14
18
22
26
30
34
S
Analytical
Numerical
r0 = 20
σ = 1

Fig. 3

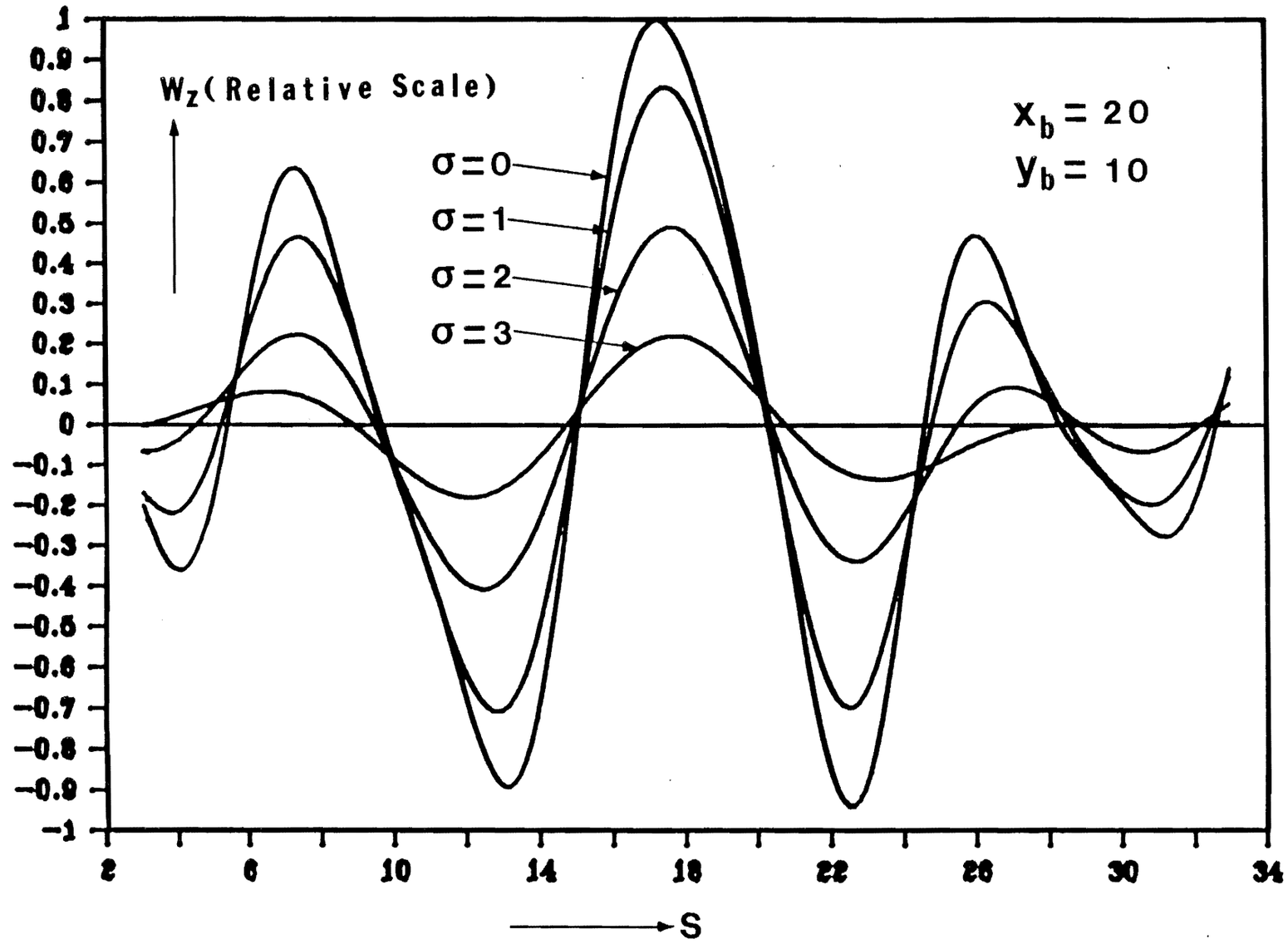
W_z(Relative Scale)
$x_b = 20$
$y_b = 10$
σ=0
σ=1
σ=2
σ=3
1
0.9
0.8
0.7
0.6
0.5
0.4
0.3
0.2
0.1
0
−0.1
−0.2
−0.3
−0.4
−0.5
−0.6
−0.7
−0.8
−0.9
−1
2
6
10
14
18
22
26
30
34
S

Fig. 4

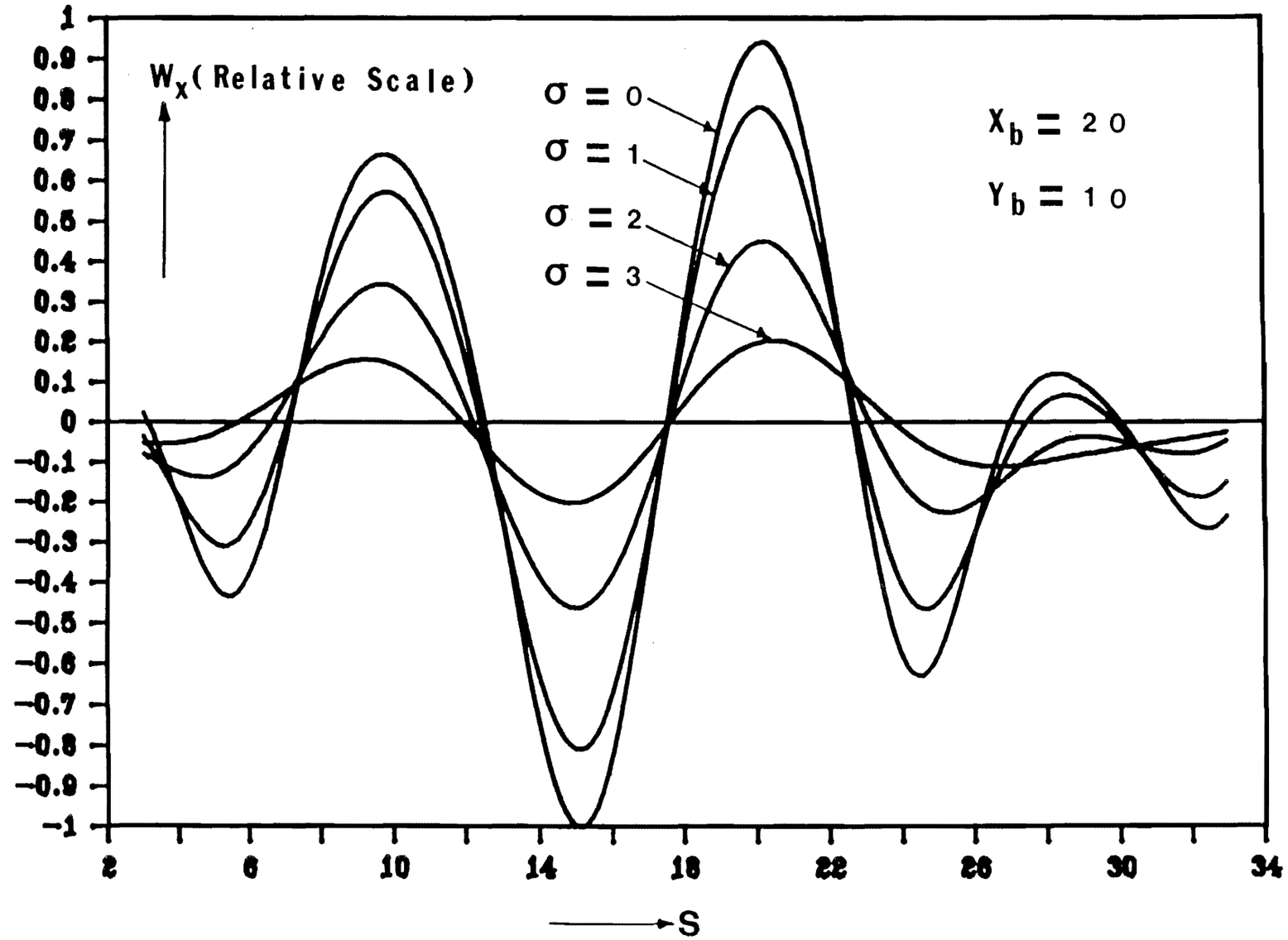
W_x (Relative Scale)
σ = 0
σ = 1
σ = 2
σ = 3
X_b = 20
Y_b = 10
1
0.9
0.8
0.7
0.6
0.5
0.4
0.3
0.2
0.1
0
-0.1
-0.2
-0.3
-0.4
-0.5
-0.6
-0.7
-0.8
-0.9
-1
2
6
10
14
18
22
26
30
34
S

Fig. 5

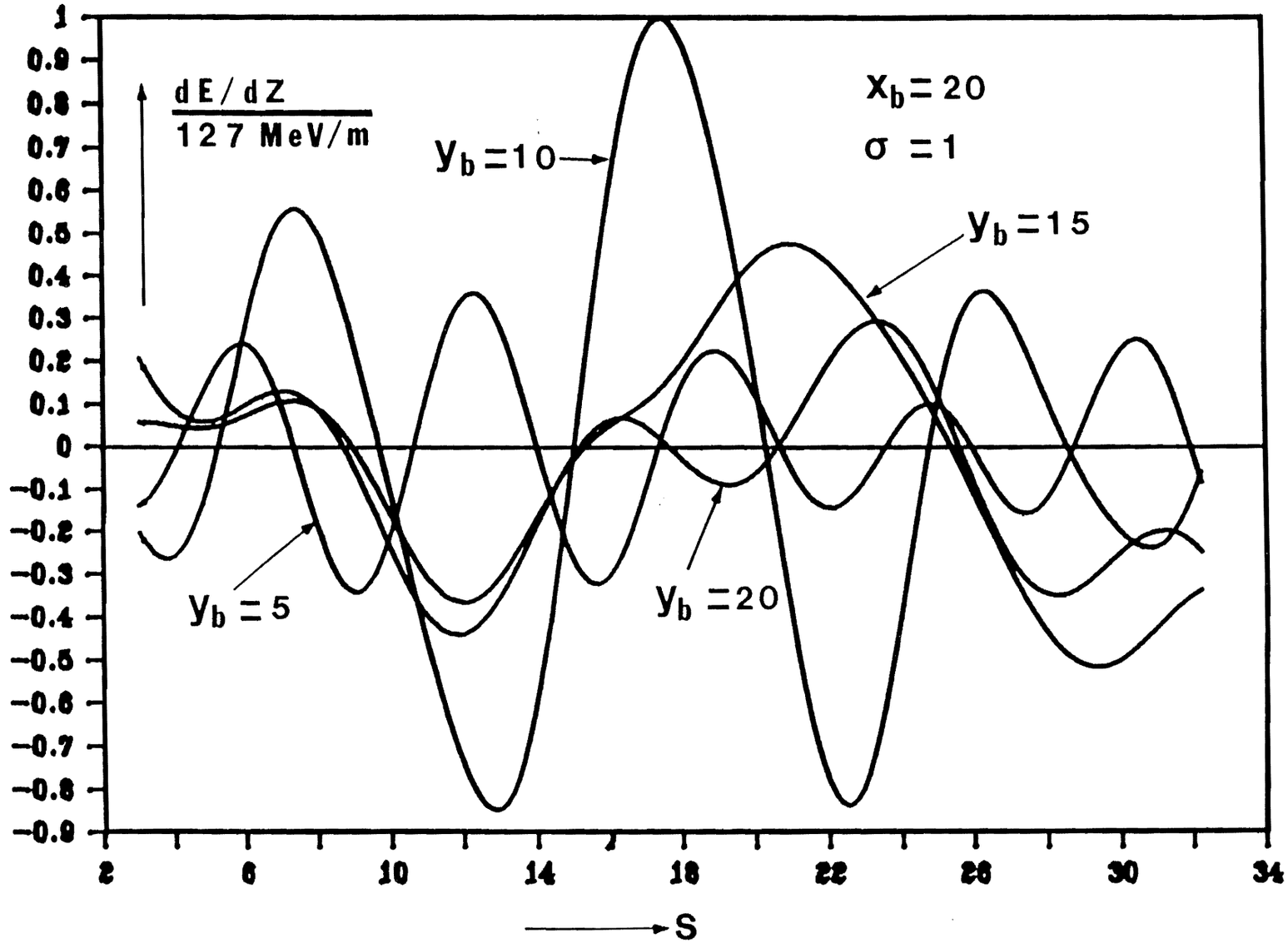
dE/dZ
127 MeV/m
$x_b = 20$
$\sigma = 1$
$y_b = 10$
$y_b = 15$
$y_b = 5$
$y_b = 20$
1
0.9
0.8
0.7
0.6
0.5
0.4
0.3
0.2
0.1
0
-0.1
-0.2
-0.3
-0.4
-0.5
-0.6
-0.7
-0.8
-0.9
2
6
10
14
18
22
26
30
34
S

Fig. 6

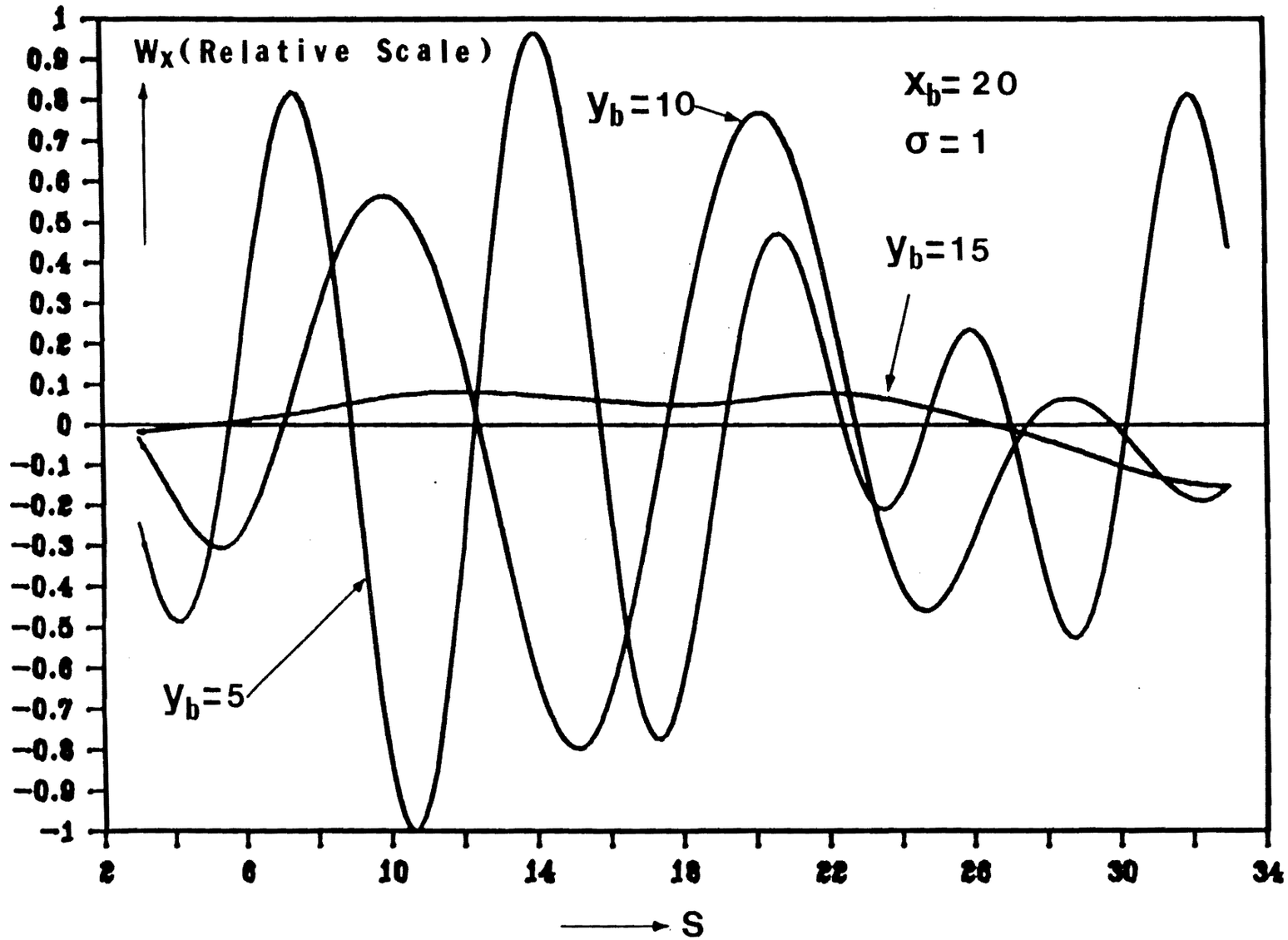
Wx(Relative Scale)
yb=10
xb= 20
σ = 1
yb=15
yb=5
1
0.9
0.8
0.7
0.6
0.5
0.4
0.3
0.2
0.1
0
-0.1
-0.2
-0.3
-0.4
-0.5
-0.6
-0.7
-0.8
-0.9
-1
2
6
10
14
18
22
26
30
34
S

Fig. 7

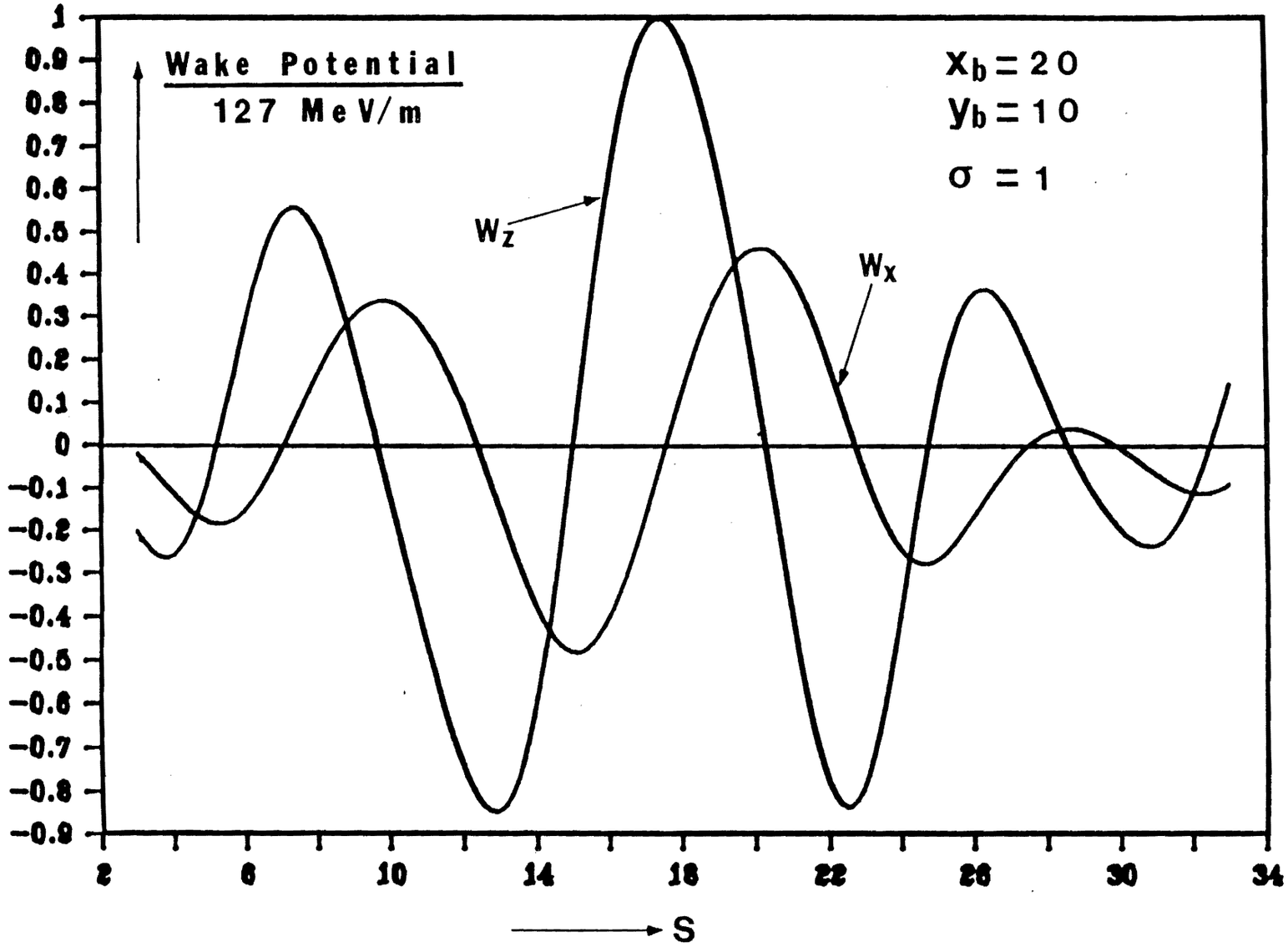
Wake Potential
127 MeV/m
$x_b = 20$
$y_b = 10$
$\sigma = 1$
W_z
W_x
1
0.9
0.8
0.7
0.6
0.5
0.4
0.3
0.2
0.1
0
−0.1
−0.2
−0.3
−0.4
−0.5
−0.6
−0.7
−0.8
−0.9
2
6
10
14
18
22
26
30
34
S

Fig. 8